Organic & Biomolecular Chemistry

ROYAL SOCIETY OF CHEMISTRY

PAPER

View Article Online
View Journal

Check for updates

Cite this: DOI: 10.1039/d4ob01539h

*cis*Pro stabilization in prolyl carbamates influenced by tetrel bonding interactions†

Shreya Banerjee,[a] Shama Tumminakatti,[a] Sudip Ghosh,[a] Vamsee K. Voora[b] and Erode N. Prabhakaran*[a]

Received 20th September 2024,
Accepted 21st October 2024

DOI: 10.1039/d4ob01539h

rsc.li/obc

NMR spectral and theoretical analyses of homologous prolyl carbamates reveal subtle charge transfer tetrel bonding interactions (TBIs), selectively stabilizing their *cis*Pro rotamers. These TBIs involve C-terminal-amide to N-terminal carbamate carbonyl–carbonyl (n → π* type) followed by intra-carbamate (n → σ* type) charge transfer interactions exclusively in the *cis*Pro motif. The number of TBIs and hence the *cis*Pro stability increase with increasing number of C^{β} groups at the carbamate alcohol. Increasing solvent polarities also increase the relative *cis*Pro carbamate stabilities.

1 Introduction

Interactions influencing *cis*Pro stability in prolyl carbamates are much less understood unlike those in prolyl amides. We know from earlier studies of homologous prolyl amides that their *cis*Pro relative stabilities and populations decrease compared to *trans*Pro, as the number of methyl substituents on the amide acyl C^{α} increases (Fig. 1a).[1,2] This is due to increasing steric clashes involving the C^{α}-substituents, which destabilize the *cis*Pro conformer more than the *trans*Pro conformer.[1,3,4] In addition to sterics, several local short-range electronic interactions, such as C_7 H-bond,[5] C_{10} H-bond[6] and C_5 O···C′ interactions,[7] also naturally favour their *trans*Pro stabilities (see the ESI, S2†) and reduce their relative *cis*Pro populations. Hence the *cis*Pro rotamers of prolyl amides have few stabilizing interactions although rare assistance from the local sequence[8–13] (see the ESI, S2†) has been observed.

A similar investigation of stereoelectronic interactions governing *cis*Pro stability in prolyl carbamates has long been lacking. We know that in carbamates, the N–C sigma bonds are largely locked in a plane due to the resonance effect at the N–C═O group[14,15] (Fig. 1b). The CO_2R group has also been shown to be locked in a plane with a predominantly cisoid geometry (Fig. 2a) due to stabilization by n → π* (ref. 16) or q → σ* (ref. 17) interactions from the carbamate carbonyl O'_C lone pair donor (D) to the π* or σ* acceptors (A) in the phenyl and alkyl substituents respectively on C^{α} of the R group. Hence, primarily the O–C^{α} and C^{α}–C^{β} σ-bonds in the R group (Fig. 1) are free to rotate. Charge transfer interactions such as n → π* and n → σ* that occur from an electron-donating Lewis base to a covalently bonded C atom acting as a Lewis acid have been referred to as tetrel bonding interactions[18,19] (TBIs).

Further investigations into stereoelectronic interactions in carbamates are essential, given the prevalence of carbamates in several bioactive peptides,[20] drugs,[21] materials[22] and fertilizers.[23] The pharmacokinetic properties of amide-based drugs, most notably their *in vivo* stability and bioavailability, have been improved by using their structural analogues – carbamates which have higher metabolic stability and cell permeability.[24] Additionally, it is possible to modulate the biological activity of carbamates by varying the substituents at the amino and carboxyl termini,[25,26] making them an integral structural and/or functional part of many drugs,[27] enzyme inhibitors,[28] and enzyme mimetics.[29]

Current systematic studies involve the synthesis and NMR spectral and theoretical analyses of homologous prolyl carbamates with increasing steric bulk on the R group (Fig. 1b) and their comparison with the corresponding homologous reference pyrrolidine models. These studies reveal an anomaly where *cis*Pro carbamate relative stabilities improve with increasing number of methyl substituents on the C^{α} of the R group. This is an inverse steric effect unlike that observed in amides (Fig. 1). DFT and NBO calculations were performed at varying C'_C–O_C–C^{α}–C^{β} (τ) torsions (Fig. 8a) which reveal the optimum geometries at which a relay of TBIs are observed predominantly in the *cis*Pro carbamate rotamers. These TBIs also stabilize the *cis*Pro conformer relative to the *trans*Pro conformer. Solvent-polarity dependent studies show the improvement of this stabilization with increasing solvent polarities.

[a]Department of Chemistry, Indian Institute of Science, Bangalore, Karnataka – 560012, India. E-mail: eprabhak@iisc.ac.in
[b]Department of Chemical Sciences, Tata Institute of Fundamental Research, Mumbai, 400005, India

† Electronic supplementary information (ESI) available. See DOI: https://doi.org/10.1039/d4ob01539h

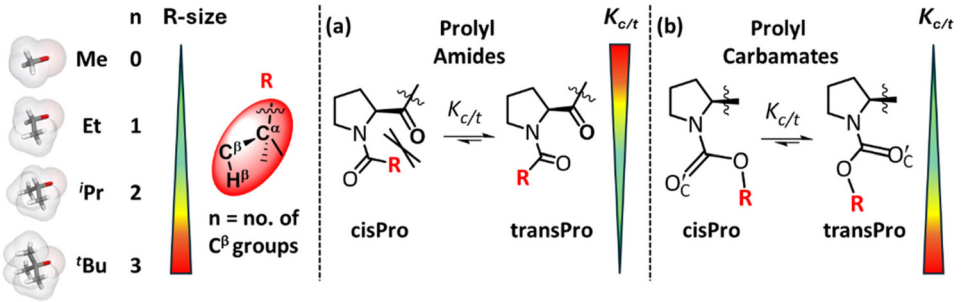

Fig. 1 Effect of increasing size of R (R = $-C^{\alpha}(C^{\beta}H_3)_nH^{\beta}{}_{3-n}$; Me → *t*Bu) on $K_{c/t}$ (equilibrium constant) for *cis*–*trans* isomerism of prolyl amides (a) and carbamates (b).

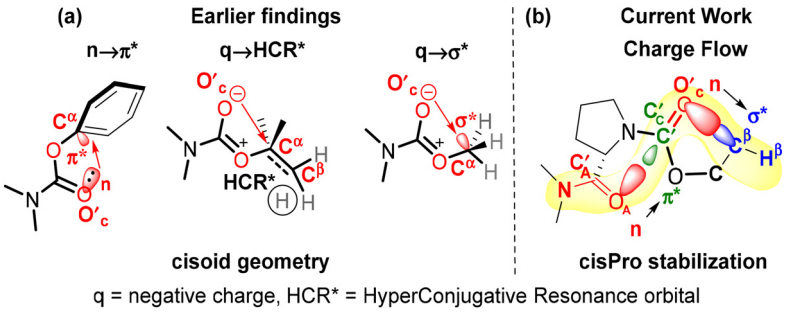

Fig. 2 (a) Earlier reports of n → π*,[16] q → HCR* (ref. 17) and q → σ* (ref. 17) interactions stabilizing the cisoid conformation of carbamates, (b) current findings of carbonyl–carbonyl (n → π* type) and intra-carbamate (n → σ* type) tetrel bonding interactions stabilizing *cis*Pro.

2 Results

The spectral signatures of charge transfer TBIs are weak and cannot be observed directly in the spectra of model compounds. For this reason, it is conventional to identify these interactions through increasing/decreasing trends of observables in homologues. Prolyl carbamate homologues **1**–**4** (Fig. 3a) were synthesized using standard solution phase synthetic protocols (see the ESI, S3 and S4†). The equilibrium constant for the *trans*Pro → *cis*Pro isomerism ($K_{c/t}$) (10 mM in

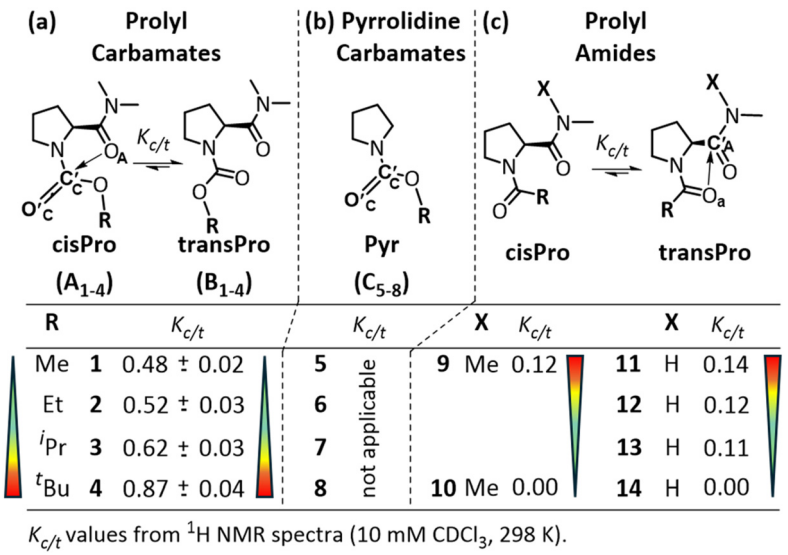

Fig. 3 *cis*/*trans* isomerism in homologous (a) prolyl carbamates (**1**–**4**), (b) corresponding pyrrolidine carbamates (**5**–**8**) and (c) prolyl amides (**9**–**14**). With increasing bulk at R, the equilibrium constant for *trans*Pro → *cis*Pro isomerism ($K_{c/t}$) increases from **1** to **4**, unlike from **9** to **10** and **11** to **14**, where they decrease.[1]

$CDCl_3$, 298 K) was determined as the ratio of the two H^{α}_{Pro} integrals in their ^{1}H NMR spectra. For the prolyl carbamate **1**, $K_{c/t}$ (0.48) is 3.6 times that of the corresponding prolyl amide **11** (0.14). This is not due to the lack of the *trans*Pro stabilizing C_7 γ-turn H-bond in **1**, because $K_{c/t}$ of **1** is 4-fold greater than that of **9** (0.12) which also lacks such an H-bond. The relatively lesser unfavorable steric clashes in the *cis*Pro rotamer of **1** due to the replacement of the bulky acyl CH_3 in **9** with a less bulky oxygen atom in **1** cannot entirely explain such a remarkable increase in $K_{c/t}$ either.

This is because, whereas $K_{c/t}$ values decrease to zero for both **10** and **14** (containing the sterically bulky ^{t}Bu substituent), it increases for **4** (compared to **1**). In fact, along the homologous carbamates **1–4**, their $K_{c/t}$ values increased from 0.48 to 0.87 with increasing steric bulk at C^{α} of the alcohol of carbamate (Fig. 3a). In contrast, the $K_{c/t}$ values of prolyl amides **9–10** and **11–14** show an opposite trend upon homologation[1] (Fig. 3c).

In pyrrolidine carbamates **5–8** (Fig. 3b), the presence of n → σ* type TBIs, from the carbamate carbonyl oxygen donor (D) to its alcohol C^{β} acceptor (A) ($O'_C \rightarrow C^{\beta}$), has been noted.[17,30,31] This increases the electrophilicity of the carbamate carbonyl carbon (C'_C) and decreases the nucleophilicity of its carbonyl oxygen, compared to the corresponding amide carbonyl. We hypothesized that the prolyl carbamate carbonyl in **1–4** could act as an electron acceptor from amide oxygen ($C'_C \leftarrow O_A$) in *cis*Pro rotamers (Fig. 3a). This would be in the reverse direction compared to **9–14** (Fig. 3c) where the oxygens of prolyl amides (O_a) are the electron donors ($O_a \rightarrow C'_A$), in the *trans*Pro rotamers.[7]

Natural Bond Orbital (NBO) analyses indicate the presence of orbital overlap interactions (1.45 kcal mol^{-1}, 1.75 kcal mol^{-1}) from two of the C–H σ orbitals in the *Z* N–CH_3 group to the σ* of the amide N–C'_A pseudo double bond in the *cis*Pro isomer of **2** (Fig. 4a). A weaker n → σ* interaction (0.78 kcal mol^{-1}) is observed in the opposite direction – from the np lone pair[32] (Fig. 4b) of the amide O_A to the σ* of the third C–H in the *Z* N–CH_3 group. Similar interactions are absent in the *trans*Pro isomer of **2**. These interactions (observed in **3** and **4** as well) indicate an overall accumulation of negative charge on the amide carbonyl carbon (C'_A) exclusively in the *cis*Pro carbamate conformers.

Investigation of the ^{13}C NMR spectrum of **1** (10 mM, $CDCl_3$) showed identical chemical shifts for the amide carbonyl carbon (C'_A) in both the *cis*Pro and *trans*Pro rotamers (Fig. 4c and d). However, the signals in *cis*Pro started to become increasingly more downfield shifted from the *trans*Pro signals in **2–4** (Fig. 4d), which contain the methyl substituents on C^{α} with their numbers increasing from one to three respectively. Such shifts occur despite the energy minimized structures of **1–4** (minimized using the B3LYP 6-311G(**)[33] basis set in Gaussian 09W[34]), showing that the amide carbonyl oxygens are not directly interacting with the carbamate C^{α} ($O_A \cdots C^{\alpha} \geq$

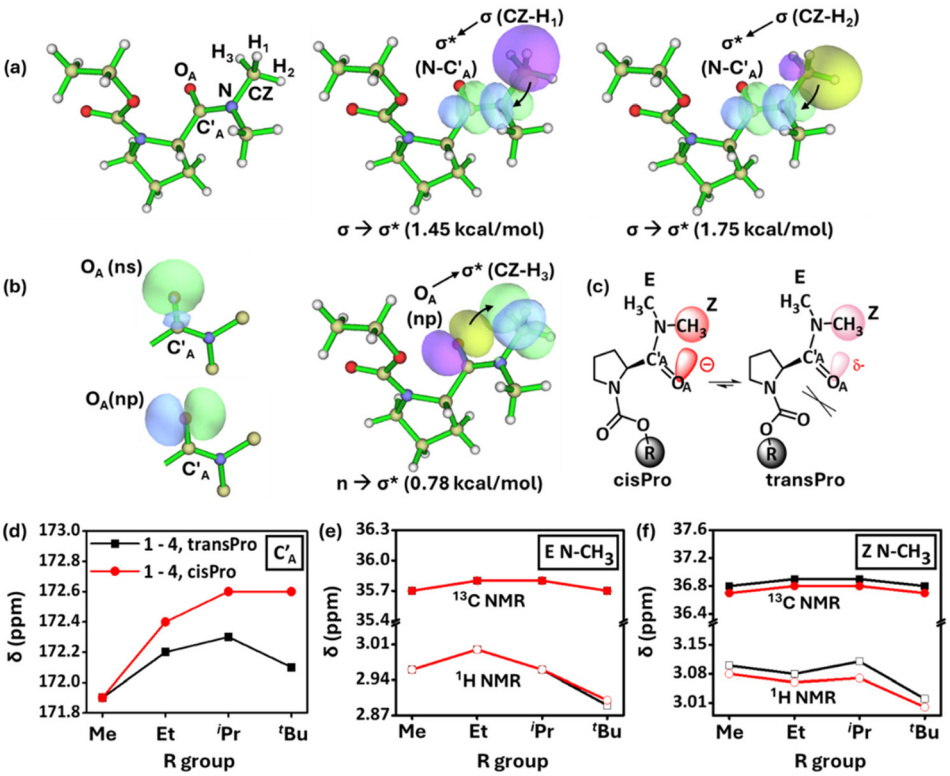

Fig. 4 (a) and (b) NBO overlap diagrams of **2** showing interaction between *Z* N–CH_3 and the amide group in the *cis*Pro isomer. ns and np orbitals of amide carbonyl O_A; (c) ChemDraw rendition showing polarization along the amide carbonyl in the *cis*Pro rotamer; plots of (d) ^{13}C δ ppm of amide carbonyl C'_A; (e and f) ^{1}H, ^{13}C δ ppm for the *E* and *Z* N–CH_3 in **1–4**, *versus* the R group of carbamates.

4.25 ± 0.15 Å), where the homologation occurs remotely (see the ESI, S9.3†).

Steric effects from homologation cannot cause such distal electronic changes. The ^{1}H and ^{13}C nuclei of *Z* N–CH_3 in the *cis*Pro rotamers of **1–4**, concomitantly, selectively get upfield shifted compared to those of *trans*Pro, unlike the *E* N–CH_3 protons where there are no such shifts (Fig. 4e and f). Clearly there is an incremental build-up of greater negative charge at the amide oxygen (O_A) selectively in the *cis*Pro rotamer, as the number of C^{β}-substituents on C^{α} increases at the remote alcohol group of carbamate from **1–4**.

This negative charge on O_A is transferred to the carbamate $C'_C{=}O'_C$ through n → π* type TBIs (Fig. 5). The charge accumulation on the carbamate C=O (C'_C, O'_C) in **1–4** was calculated from the DFT-optimized structures using the B3LYP 6-311G(**)[33] basis set in Gaussian 09W.[34] With the increase in the number of C^{α}-substituents in **1–4**, there is an increase in negative charge on O'_C (Fig. 5b) and a corresponding increase in the positive charge on C'_C exclusively in the *cis*Pro isomer. Note that there is no direct orbital overlap between the amide and carbamate groups (Fig. 5a), which indicates that this charge transfer is a through-space effect. There is no such charge transfer observed in the *trans*Pro isomer (Fig. 5b and c) where the carbamate $C'_C{=}O'_C$ dipole remains similar in **1–4**. Although the $C'_A{=}O_A{\cdots}C'_C{=}O'_C$ distance is longer (3.29 ± 0.03 Å) than the Bürgi–Dunitz distances necessary for n → π* orbital overlap,[35] in both *cis*Pro and *trans*Pro, the angle of incidence $\angle O_A{\cdots}C'_C{=}O'_C$ is within that prescribed trajectory (105.3°–133.7°)[36] exclusively in *cis*Pro (130.5° ± 0.52°) unlike in *trans*Pro (91.80° ± 0.36°).

Consistent with the results of the NBO analyses, there is upfield shifting of the charge acceptor carbamate C'_C ^{13}C NMR chemical shifts in **1–4** selectively in *cis*Pro, compared to their *trans*Pro (Fig. 6a and b) and their corresponding reference pyrrolidine models **5–8** ($\Delta\delta$ = 0.8 ± 0.2 ppm) where there is no C-terminal amide group to act as a charge donor. The ^{13}C NMR signals of *trans*Pro carbamate C'_C in **1–4** were nearly identical to those of pyrrolidine models **5–8** ($\Delta\delta$ = 0.2 ± 0.1 ppm). Hence the selective subtle shielding and increase in electron density of *cis*Pro carbamate C'_C is due to carbonyl amide ($C'_A{=}O_A$) → carbonyl carbamate ($C'_C{=}O'_C$) ($C'_AO_A{\cdots}C'_CO'_C$) charge transfer TBIs – which are largely absent in *trans*Pro.

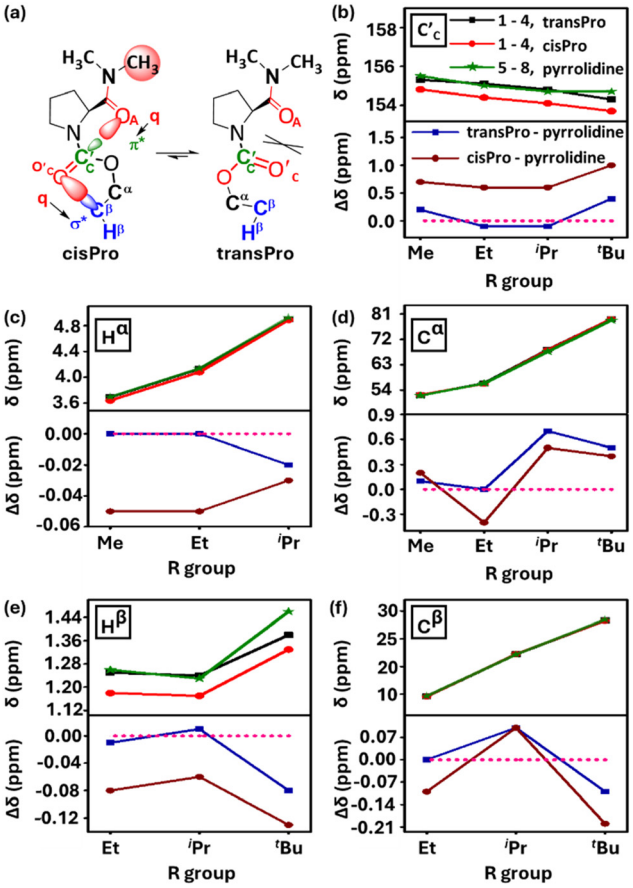

Fig. 6 (a) ChemDraw images highlighting the H^{α}, H^{β}, C^{α}, C^{β} nuclei in carbamate alcohol; (b–f) plots of ^{13}C and ^{1}H NMR (10 mM, $CDCl_3$, 298 K) chemical shifts (δ ppm) for carbamate carbonyl C'_C and for H^{α}, H^{β}, C^{α}, C^{β} of carbamate alcohol in **1–4** and **5–8** *versus* the R group of carbamates and their difference of chemical shifts from *trans*Pro & *cis*Pro rotamers (**1–4**) to pyrrolidine (**5–8**) ($\Delta\delta$ ppm).

These relatively small $\Delta\delta$ ppm values observed for C′ and N–CH_3 are reliable and indicate perturbations from the charge relay interactions and are not resulting from mere conformational anisotropies. This is because the $\Delta\delta$ ppm values of the prolyl ring protons (H^{β}, H^{γ}) and carbons (C^{β}, C^{γ}) between

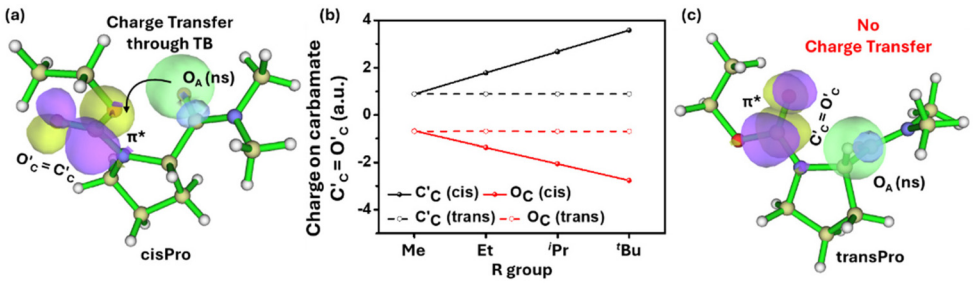

Fig. 5 NBO diagrams in the *cis*Pro (a) and *trans*Pro (c) isomers of **2** showing the presence of charge transfer from amide O_A to carbamate $C'_C{=}O'_C$ selectively in *cis*Pro. (b) Plot of net charge on carbamate carbonyl in *cis*Pro and *trans*Pro (C'_C, O'_C) as a function of increasing size of the R group in carbamates (Me to ^{t}Bu, **1–4**).

the *cis*Pro and *trans*Pro rotamers of **1–4** are ~0.00 ppm (see the ESI, S6.6 and S6.7†). However, for the C^{α}, H^{α} and C^{β}, H^{β} of the Pro ring, which directly interact with the different charge environments in *cis*Pro and *trans*Pro rotamers, the $\Delta\delta$ ppm values are non-zero (Fig. 6c–f). Additionally, concentration dependent FT-IR and NMR studies (see the ESI, S7†) showed no variance at all in any of the vibrational bands and chemical shifts of any of the nuclei, indicating that the observed spectral shifts are not due to intermolecular associations either.

NBO analyses[7,32] of the energy minimized (using the B3LYP 6-311G(**)[33] basis set in Gaussian 09W[34]) structures of **1–4** showed no orbital overlaps (zero energies) between the lone pair of amide oxygen and π* of carbamate C'_C in the *cis*Pro or *trans*Pro rotamers (see the ESI, S9.4†). The shortest possible $O_A\cdots C'_C$ distances, derived from energy minimized structures, are also longer (3.29 ± 0.03 Å) than the Bürgi–Dunitz distances necessary for n → π* orbital overlap interactions.[7,35] The weak $C'_AO_A\cdots C'_CO'_C$ interactions in *cis*Pro evidenced by the NMR spectral markers thus involve charge transfer TBIs and not orbital overlaps (n → π*). In *trans*Pro, the two carbonyls are not oriented suitably to favour such charge transfer, but their oxygens are close (3.49 ± 0.03 Å) to experience Pauli repulsions (Fig. 6a). Hence similar TBIs are unavailable in *trans*Pro, due to which its spectral shifts are similar to those of the pyrrolidine models **5–8** that lack the charge donor amide group.

The FT-IR spectra (10 mM, $CHCl_3$) showed a net decrease in carbamate C═O stretching frequency and a net increase in amide C═O stretching frequency from **1–4** (see the ESI, S6.8†). The relatively low correlation between the stretching frequencies (χ^2 = 0.74) is expected since *cis*Pro, where most of the subtle spectral variations occur, is the minor rotamer. However, the slope of the observed correlation suggests about a two-fold increase in the carbamate C═O stretch concomitant to a unit decrease in the amide C═O stretch, as the number of σ* acceptors increases (Fig. 7b), which is another spectral observable for the charge transfer $C'_AO_A\cdots C'_CO'_C$ interactions.

The consequence of the greater negative charge build-up at the carbamate oxygen (O'_C) selectively in the *cis*Pro rotamers of **1–4** is seen in the upfield shifts of their carbamate ester H^{α} and C^{α} NMR signals (compared to both *trans*Pro and pyrrolidine **5–8**). Notably, the H^{β} and C^{β} of *cis*Pro also shift upfield (Fig. 6c–f). The formation of intramolecular 5- and 6-membered H-bonds of the type O···H–C is unlikely, as it would have caused upfield shifts in H^{α}, H^{β} and downfield shifts in C^{α}, C^{β} due to polarization of the C–H bond.[37] On the other hand, perturbation of the intra-carbamate TBIs along O → C^{β}–H^{β} by the charge transfer from the carbamate oxygen (Fig. 7a) is more consistent with the observed shifts. Indeed, DFT optimized structures of the *cis*Pro isomer of **1–4** showed only O → C^{β}–H^{β} and no O → C^{α}–H^{α}/C^{α}–C^{β} interactions (Fig. 8).

To determine the torsion angle τ_{min} (τ = C'_C–O_C–C^{α}–C^{β}) at which there is maximum stabilization from carbonyl–carbonyl (n → π*) TBIs and intra-carbamate (n → σ*) TBIs in *cis*Pro and *trans*Pro of **1–4**, an energy screening at different torsion angles was performed as follows. τ was varied from −180° to +180° in steps of 1°–30° (as necessary) and the structure was allowed to optimize at each value of τ (Fig. 8a) using the B3LYP 6-311G (**)[33] basis set in Gaussian 09W.[34] Second order perturbation energies $E(2)$ for the optimized structures were calculated for the *cis*Pro and *trans*Pro isomers of **1–4** from these DFT-optimized structures.

These $E(2)$ energies were normalized for comparison between homologues as follows. The n → σ* TBI energies in **1–4** contain two components: (a) one that is due to any n → σ* TBIs that are inherent in the carbamate (inherent n → σ*) in the absence of any n → π* TBIs and (b) another that is due to any changes induced in these n → σ* TBIs (induced n → σ*) by the presence of the n → π* TBIs. Hence, **1–4** contain the total energies due to three TBIs: (a) n → π*; (b) inherent n → σ*; and (c) induced n → σ*. Reference models **5–8** contain exclusively the inherent n → σ* TBIs. Note that these inherent TBI energies would vary with the homologation of the alcohol group in the carbamates. The energies of these inherent n → σ* TBIs in **5–8** (as a function of τ) were hence subtracted from the total (n → π* + inherent n → σ* + induced n → σ*) TBI energies of *cis*Pro and *trans*Pro in **1–4** to give their normalized $E(2)$ values (Fig. 8b).

In the plot of $E(2)$ *vs.* τ, two sharp non-zero energy minima are observed, one each at positive and negative values of τ (termed τ_{min}), for both the *cis*Pro and *trans*Pro sets. This is expected because there are two *gauche* ranges of τ around the carbamate C═O (τ = 0° to −60°, 0° to 60°) (Fig. 8a) where the

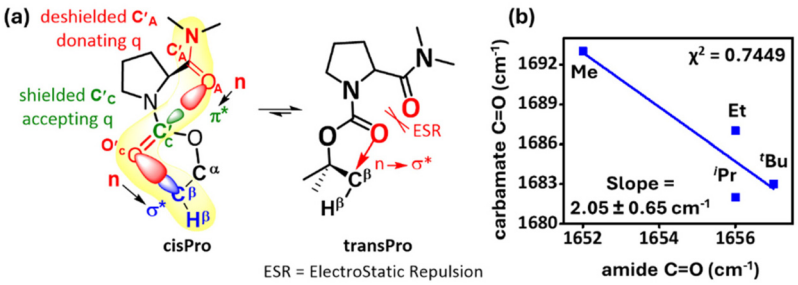

Fig. 7 (a) Summary of spectral observations revealing charge transfer through carbonyl–carbonyl and intra-carbamate TBIs at *cis*Pro carbamates. ESR interactions perturb *trans*Pro carbamates; (b) correlation plot between amide and carbamate FT-IR C═O stretch bands of donor (*x*-axis) /acceptor (*y*-axis) carbonyls.

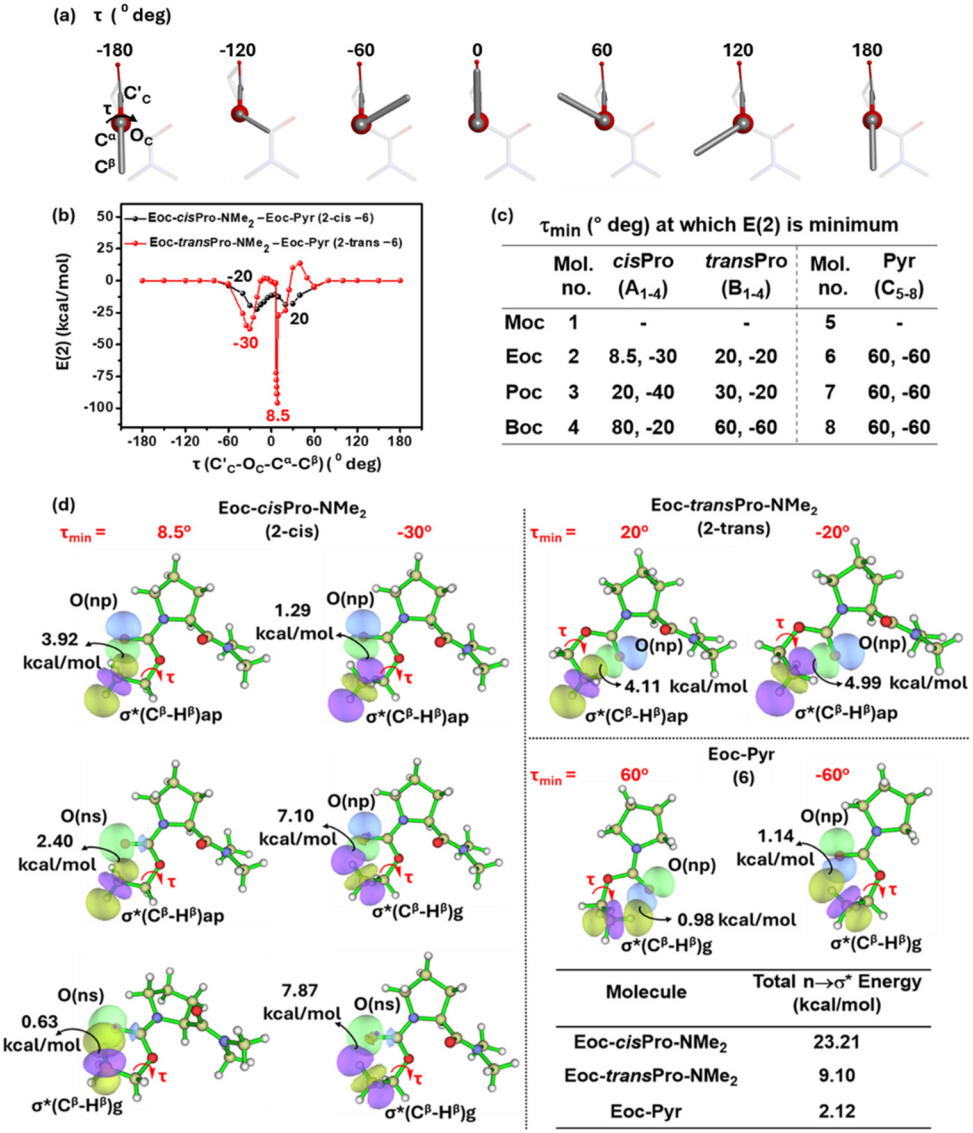

	Mol. no.	*cis*Pro (A_{1-4})	*trans*Pro (B_{1-4})	Mol. no.	Pyr (C_{5-8})
Moc	1	-	-	5	-
Eoc	2	8.5, -30	20, -20	6	60, -60
Poc	3	20, -40	30, -20	7	60, -60
Boc	4	80, -20	60, -60	8	60, -60

Molecule	Total n→σ* Energy (kcal/mol)
Eoc-*cis*Pro-NMe_2	23.21
Eoc-*trans*Pro-NMe_2	9.10
Eoc-Pyr	2.12

Fig. 8 (a) Rotational scan of energy over the entire range of τ (C'_C–O_C–C^α–C^β). (b) Variation of normalized second-order perturbation energy $E(2)$ with τ in Eoc-*cis*Pro-NMe_2 and Eoc-*trans*Pro-NMe_2 (**2**). (c) Table of τ_{min} values of **1–4**, **5–8**. (d) NBO overlap diagrams showing the energy of each interaction. The net energies are tabulated. (Moc methyloxycarbonyl, Eoc ethyloxycarbonyl, Poc isopropyloxycarbonyl, Boc *tert*-butyloxycarbonyl).

σ* of the C^β–H^β is in a suitable orientation for n → σ* type TBIs (except in **1**). In **1** there are no C^β substituents and hence no such charge transfer can occur. The τ_{min} values of **2** where $E(2)$ is minimum are shown (Fig. 8b and c) and are representative of **3** and **4**. The τ_{min} values for *cis*Pro are asymmetrically distributed about zero and have much lower $E(2)$ values compared to *trans*Pro, whose $E(2)$ values are symmetrical about zero and are shallower (Fig. 8b).

Closer examination showed that *cis*Pro of **2** has three TBIs in the −ve and +ve τ values each, where NBO analyses show that D → A (donor → acceptor) orbital overlap (one np → σ* and two ns → σ*; σ* of C^β–H^β) interactions happen (Fig. 8d). Their corresponding $O'_C \cdots C^\beta$ distances are 2.86 ± 0.05 Å (Fig. 9) which are also well within the threshold range (3.22 Å)[38,39] for O···C non-covalent interactions. These are consistently observed in *cis*Pro of **3** and **4** as well (Fig. 9).

On the other hand, in *trans*Pro of **1–4** although the $O'_C \cdots C^\beta$ (Å) and τ magnitudes (Fig. 9) are conducive for D → A interactions and there are two τ_{min} values where O'_C → C^β interactions do occur (Fig. 8d), in both of them, there is only one np → σ* type TBI each. Notably the net NBO overlap energy in *trans*Pro is significantly lower than that in *cis*Pro (Fig. 8d). Hence, the n → σ* type TBIs predominate in the *cis*Pro conformers, and their energies improve relative to *trans*Pro with increasing number of σ* acceptors (of C^β–H^β). As a result, there is anomalous *cis*Pro stabilization from Moc to Boc (**1** to **4**) despite the concomitant increase in steric bulk at R of the CO_2R group in these carbamates.

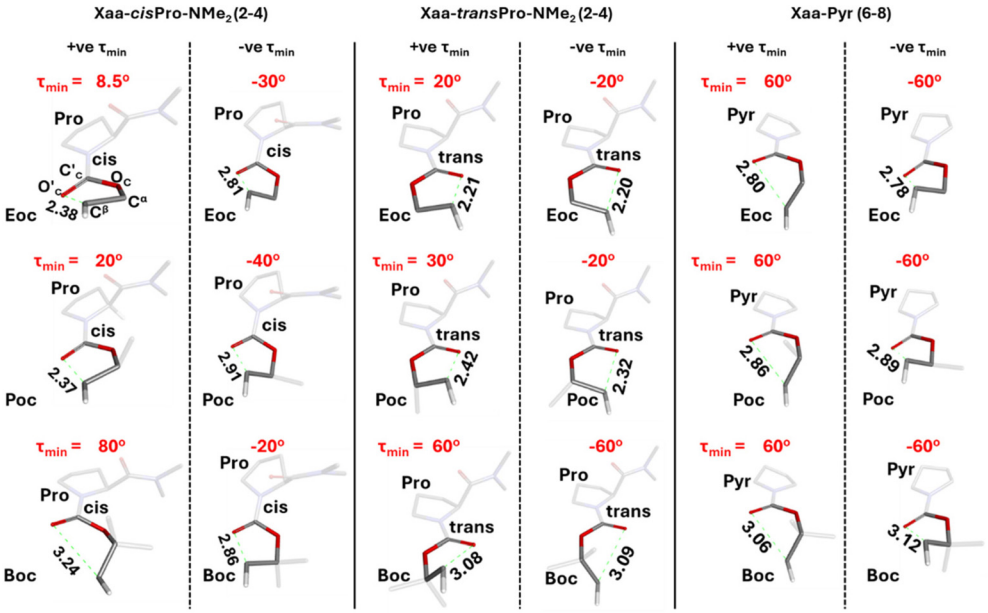

Fig. 9 The pseudo-five-membered ring formed by the n → σ* type TBIs is shown for the *cis*Pro and *trans*Pro isomers of all the homologues (**2**, **3**, **4**) and their corresponding pyrrolidine analogues (**6**, **7**, **8**). The green dotted lines depict the $O'_C \cdots C^\beta$ interactions. All structures are at their respective τ_{min} (the dihedral angle $C'_C–O_C–C^\alpha–C^\beta$ at which energy of n → σ* type TBI is minimum).

In order to investigate the reason for the asymmetry of τ_{min} (about 0) exclusively in *cis*Pro of **2–4**, the geometries of their carbamate groups in *cis*Pro and *trans*Pro were compared. At τ_{min} in *cis*Pro of **2–4**, the $O'_C \cdots C^\beta$ TBIs (depicted as green dotted lines in Fig. 9) result in the formation of a pseudo five-membered ring which adopts a half-chair conformation (Fig. 10)[40] with O'_C oriented *exo* and C^β-*endo*, with respect to the proline substituent (Fig. 10) on the $C'_C–O_C–C^\alpha$ plane.[41] The two H^αs on C^α in **2** are pseudo-equatorially (e′) and pseudo-axially (a′) oriented (Fig. 10). In **3**, the $C^\beta H_3$ group that replaces one of the H^α occupies e′.[42] In **4**, both e′ and a′ are occupied by $C^\beta H_3$ groups. There is significant out of plane puckering of the

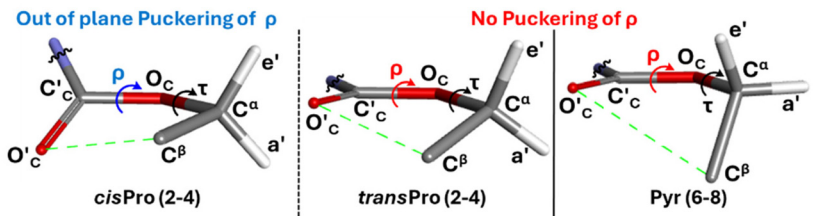

		Xaa-*cis*Pro-NMe$_2$		Xaa-*trans*Pro-NMe$_2$		Xaa-Pyr	
	Torsion (° deg)	Xaa = Eoc (**2**)		Xaa = Eoc (**2**)		Xaa = Eoc (**6**)	
τ_{min}	C'_C-O_C-C^α-C^β	8.5	-30.0	20.1	-20.0	60.0	-60.0
ρ	**O'_C=C'_C-O_C-C^α**	-44.9	-44.9	1.1	1.1	0.9	0.8
	Torsion (° deg)	Xaa = Poc (**3**)		Xaa = Poc (**3**)		Xaa = Poc (**7**)	
τ_{min}	C'_C-O_C-C^α-C^β	20.0	-40.0	30.0	-20.0	60.0	-60.0
ρ	**O'_C=C'_C-O_C-C^α**	-34.8	-34.9	-0.1	0.0	-2.0	-2.0
	Torsion (° deg)	Xaa = Boc (**4**)		Xaa = Boc (**4**)		Xaa = Boc (**8**)	
τ_{min}	C'_C-O_C-C^α-C^β	80.0	-20.1	60.0	-60.0	60.0	-60.0
ρ	**O'_C=C'_C-O_C-C^α**	-40.4	-40.4	2.9	2.9	0.7	0.7

Fig. 10 The pseudo-five-membered ring formed by the n → σ* type TBIs interactions is shown for the *cis*Pro and *trans*Pro isomers of **2** along with the corresponding pyrrolidine analogue **6**. The ρ torsions (O'_C=$C'_C–O_C–C^\alpha$) are tabulated corresponding to the value at τ_{min} (the dihedral angle $C'_C–O_C–C^\alpha–C^\beta$ at which energy of n → σ* type TBI is minimum).

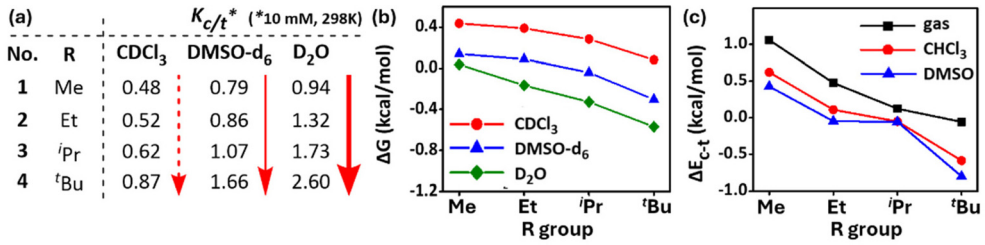

Fig. 11 (a) $K_{c/t}$ values of **1–4** in different solvents (10 mM, 298 K); plots of (b) experimental and (c) theoretically calculated conformational energy differences between *trans*Pro and *cis*Pro isomers in **1–4** in different solvents (298 K).

torsion ρ ($O'_c{=}C'_C{-}O_C{-}C^\alpha$, Fig. 10) by −40.0 ± 5.0° to accommodate the $O'_C \rightarrow C^\beta$ interactions in both the positive and negative τ_{min} selectively in the *cis*Pro isomers in **2–4**.

Contrarily, in *trans*Pro of **2–4** as well as in the reference pyrrolidine models **6–8** – that lack the $C'_A{=}O_A$ charge donor source – there are no n → σ* type TBIs ($O'_C \rightarrow C^\beta$) at τ_{min}, as indicated by the absence of the ρ-puckering (Fig. 10). In both **2–4** and **6–8**, the $O'_C{=}C'_C{-}O_C{-}C^\alpha$ group is largely in plane, indicating much less perturbation by any charge transfer unlike in *cis*Pro. These selective puckering effects at the *cis*Pro carbamate CO_2R group are hence the steric consequences of the $O'_C{\cdots}C^\beta$ (n → σ*) TBIs which occur predominantly in the *cis*Pro rotamers and cause the observed asymmetry of τ_{min}.

Thus, a combination of two TBIs, one originating from the prolyl C-terminal amide oxygen (O_A) to its N-terminal carbamate carbon (C'_C) through carbonyl–carbonyl ($O_A \rightarrow C'_C$) n → π* type interactions and the other from the carbamate oxygen (O'_C) to the σ* of the $C^\beta{-}H^\beta$ bond through intra-carbamate n → σ* type interactions, predominantly occurs in the *cis*Pro conformers of prolyl carbamates and selectively stabilizes them compared to their *trans*Pro rotamers. Their interaction energies improve with increasing number of $C^\beta H_3$ substituents in the carbamate R group.

To observe the effect of solvent on these *cis*Pro stabilizing TBIs, the $K_{c/t}$ (Fig. 11a) and corresponding ΔG (kcal mol^{-1}) (Fig. 11b) values (10 mM, 298 K, calculated using the Gibbs free energy equation $\Delta G = -RT \ln K_{c/t}$) of **1–4** were recorded in more polar solvents (DMSO-d_6, D_2O). The $K_{c/t}$ and ΔG values of **1–4** improved as the solvent polarity increased ($CDCl_3$ < DMSO-d_6 < D_2O). Notably, $K_{c/t}$ of **4** shows a remarkable value of 2.60 (Fig. 10a) (ΔG = −0.56 kcal mol^{-1}; >72% *cis*Pro carbamate!) in aqueous medium (10% DMSO-d_6 was added to D_2O to improve solubility). To understand the source of such *cis*Pro stabilization, studies were conducted to calculate the theoretical free energy difference ΔE_{c-t} (corresponding to experimental ΔG) values of **1–4** with the PBE functional[43] and def2-TZVPP basis sets using the TURBOMOLE V7.5 software.[44]

They showed similar trends for ΔE_{c-t} (kcal mol^{-1}) of **1–4** in the gas phase ($\Delta E_{c-t} = E_{cis\text{Pro}} - E_{trans\text{Pro}}$; more negative value for ΔE_{c-t} implies greater stabilization of *cis*Pro) (Fig. 10c). Importantly, when solvation effects were included *via* the COSMO solvation model,[45] the theoretical ΔE_{c-t} values also adopt more negative values with increasing solvent polarities (gas < $CHCl_3$ < DMSO) (Fig. 10c). These data reveal better relative stabilization of *cis*Pro containing the charge transfer TBIs in solvents of higher polarity. Hence, solvation effects also contribute significantly to *cis*/*trans* free energy differences in prolyl carbamates.

3 Conclusions

In this work, the conformations of *cis*Pro and *trans*Pro rotamers of homologous prolyl carbamates and their corresponding pyrrolidine carbamates were investigated using NMR and theoretical (DFT, NBO) methods. These studies reveal an anomaly, where the relative stabilities of *cis*Pro carbamates are found to increase with increasing steric bulk at R of the carbamate CO_2R group. We observe the presence of a relay of two charge transfer tetrel bonding interactions (TBIs) predominantly in *cis*Pro carbamates, which also stabilise them. First a charge transfer occurs from the amide oxygen to the carbamate carbon both of which flank the proline, through a carbonyl–carbonyl n → π* type TBI. This charge is further transferred from the carbamate oxygen to the σ* of the $C^\beta{-}H^\beta$ bond (in $C({=}O)O{-}C^\alpha{-}C^\beta{-}H^\beta$ of the carbamate alcohol group) through an intra-carbamate n → σ* type TBI. Energies of the latter TBI improve with increase in the number of σ* acceptors (of $C^\beta{-}H^\beta$), despite the concomitant increase in steric bulk at the carbamate alcohol. This charge transfer relay of TBIs occurring in *cis*Pro of prolyl carbamates is in the reverse direction (C-terminal to N-terminal across Pro) compared to that observed in *trans*Pro of prolyl amides (N-terminal to C-terminal across Pro) – both of which stabilize their corresponding conformers. A consequence of the stronger TBIs in *cis*Pro carbamates is that there is significant puckering in the $O'_c{=}C'_C{-}O_C{-}C^\alpha$ (−40 ± 5°) torsion of the pseudo five-membered rings formed at the $C({=}O)O{-}C^\alpha{-}C^\beta{-}H^\beta$ group of carbamates. Increasing solvent polarities are observed to further improve the relative stabilities of *cis*Pro carbamate conformers. This work provides first insights into the tetrel interactions that govern the *cis–trans* isomerism in carbamates. Given that carbamates appear in several biorelevant molecules[46] and their *cis–trans* isomerism has been used to regulate ion flux in artificial ion channels,[47] the current results are also important

in showcasing the alcohol groups of carbamates as tools to regulate their *cis–trans* equilibria to suit various applications.

Data availability

The data supporting this article have been included as part of the ESI.†

Conflicts of interest

There are no conflicts to declare.

References

1 D. N. Reddy and E. N. Prabhakaran, Steric and electronic interactions controlling the cis/trans isomer equilibrium at X-pro tertiary amide motifs in solution, *Biopolymers*, 2014, **101**(1), 66–77.
2 G.-B. Liang, C. J. Rito and S. H. Gellman, Variations in the turn-forming characteristics of N-Acyl proline units, *Biopolymers*, 1992, **32**(3), 293–301.
3 D. N. Reddy, G. George and E. N. Prabhakaran, Crystal-Structure Analysis of cis-X-Pro-Containing Peptidomimetics: Understanding the Steric Interactions at cis X-Pro Amide Bonds, *Angew. Chem., Int. Ed.*, 2013, **52**(14), 3935–3939.
4 S. Banerjee, S. K. Gupta, S. Pal and E. N. Prabhakaran, Crystal structures reveal that the sterically hindered pivaloyl–cisProlyl amide bond is energetically frustrated, *Pept. Sci.*, 2024, **116**(3), e24337.
5 C. Rao, P. Balaram and C. Rao, Infrared spectroscopic study of C7 intramolecular hydrogen bonds in peptides, *Biopolymers*, 1983, **22**(9), 2091–2104.
6 B. N. Rao, A. Kumar, H. Balaram, A. Ravi and P. Balaram, Nuclear Overhauser effects and circular dichroism as probes of. beta.-turn conformations in acyclic and cyclic peptides with pro-X sequences, *J. Am. Chem. Soc.*, 1983, **105**(25), 7423–7428.
7 A. Choudhary, C. G. Fry, K. J. Kamer and R. T. Raines, An n→ π* interaction reduces the electrophilicity of the acceptor carbonyl group, *Chem. Commun.*, 2013, **49**(74), 8166–8168.
8 N. J. Zondlo, Aromatic–Proline Interactions: Electronically Tunable CH/π Interactions, *Acc. Chem. Res.*, 2013, **46**(4), 1039–1049.
9 B. Dasgupta, P. Chakrabarti and G. Basu, Enhanced stability of cis Pro-Pro peptide bond in Pro-Pro-Phe sequence motif, *FEBS Lett.*, 2007, **581**(23), 4529–4532.
10 S. K. Gupta, S. Banerjee and E. N. Prabhakaran, van der Waals interactions to control amide cis–trans isomerism, *New J. Chem.*, 2022, **46**(26), 12470–12473.
11 H. K. Ganguly, B. Majumder, S. Chattopadhyay, P. Chakrabarti and G. Basu, Direct Evidence for CH···π Interaction Mediated Stabilization of Pro-cisPro Bond in Peptides with Pro-Pro-Aromatic motifs, *J. Am. Chem. Soc.*, 2012, **134**(10), 4661–4669.
12 S. Banerjee, S. K. Gupta and E. N. Prabhakaran, Direct Evidence for Synchronicity between Rotation along Cα–C′ and Pyramidalization of C′ in Amides, *ChemistrySelect*, 2023, **8**(17), e202301105.
13 S. Banerjee, S. K. Gupta, S. Pal and E. N. Prabhakaran, Crystal structures reveal that the sterically hindered pivaloyl–cisProlyl amide bond is energetically frustrated, *Pept. Sci.*, 2024, e24337.
14 C. M. Lee and W. Kumler, The dipole moment and structure of the carbamate group, *J. Am. Chem. Soc.*, 1961, **83**(22), 4596–4600.
15 M. J. Deetz, C. C. Forbes, M. Jonas, J. P. Malerich, B. D. Smith and O. Wiest, Unusually low barrier to carbamate C–N rotation, *J. Org. Chem.*, 2002, **67**(11), 3949–3952.
16 B. Sahariah and B. K. Sarma, Spectroscopic evidence of n→ π* interactions involving carbonyl groups, *Phys. Chem. Chem. Phys.*, 2020, **22**(46), 26669–26681.
17 E. N. Prabhakaran, S. Tumminakatti, K. Vats and S. Ghosh, Spectral evidence for generic charge→ acceptor interactions in carbamates and esters, *RSC Adv.*, 2020, **10**(20), 11871–11875.
18 S. Scheiner, Origins and properties of the tetrel bond, *Phys. Chem. Chem. Phys.*, 2021, **23**(10), 5702–5717.
19 V. L. Heywood, T. P. Alford, J. J. Roeleveld, S. J. L. Deprez, A. Verhoofstad, J. I. van der Vlugt, S. R. Domingos, M. Schnell, A. P. Davis and T. J. Mooibroek, Observations of tetrel bonding between sp 3-carbon and THF, *Chem. Sci.*, 2020, **11**(20), 5289–5293.
20 T. Yoshimoto, K. Kawahara, F. Matsubara, K. Kado and D. Tsuru, Comparison of inhibitory effects of prolinal-containing peptide derivatives on prolyl endopeptidases from bovine brain and Flavobacterium, *J. Biochem.*, 1985, **98**(4), 975–979.
21 A. Dal Corso, V. Borlandelli, C. Corno, P. Perego, L. Belvisi, L. Pignataro and C. Gennari, Fast Cyclization of a Proline–Derived Self–Immolative Spacer Improves the Efficacy of Carbamate Prodrugs, *Angew. Chem.*, 2020, **132**(10), 4205–4210.
22 J. Shi, T. Zheng, Y. Zhang, B. Guo and J. Xu, Cross-linked polyurethane with dynamic phenol-carbamate bonds: properties affected by the chemical structure of isocyanate, *Polym. Chem.*, 2021, **12**(16), 2421–2432.
23 N. J. Baker, B. A. Bancroft and T. S. Garcia, A meta-analysis of the effects of pesticides and fertilizers on survival and growth of amphibians, *Sci. Total Environ.*, 2013, **449**, 150–156.
24 R. Karaman, Prodrugs Design Based on Inter–and Intramolecular Chemical Processes, *Chem. Biol. Drug Des.*, 2013, **82**(6), 643–668.
25 D. Chaturvedi, Perspectives on the synthesis of organic carbamates, *Tetrahedron*, 2012, **68**(1), 15–45.
26 A. K. Ghosh and M. Brindisi, Organic carbamates in drug design and medicinal chemistry, *J. Med. Chem.*, 2015, **58**(7), 2895–2940.

27 A. Matošević and A. Bosak, Carbamate group as structural motif in drugs: A review of carbamate derivatives used as therapeutic agents, *Arh. Hig. Rada Toksikol.*, 2020, **71**(4), 285–299.
28 J. C. Verheijen, K. A. Wiig, S. Du, S. L. Connors, A. N. Martin, J. P. Ferreira, V. I. Slepnev and U. Kochendörfer, Novel carbamate cholinesterase inhibitors that release biologically active amines following enzyme inhibition, *Bioorg. Med. Chem. Lett.*, 2009, **19**(12), 3243–3246.
29 A. B. Smith III, A. K. Charnley and R. Hirschmann, Pyrrolinone-Based peptidomimetics."Let the enzyme or receptor be the judge", *Acc. Chem. Res.*, 2011, **44**(3), 180–193.
30 S. K. Singh, K. K. Mishra, N. Sharma and A. Das, Direct spectroscopic evidence for an n→ π* interaction, *Angew. Chem., Int. Ed.*, 2016, **55**(27), 7801–7805.
31 S. K. Singh, P. Panwaria, K. K. Mishra and A. Das, Steric as well as n→ π* Interaction Controls the Conformational Preferences of Phenyl Acetate: Gas–phase Spectroscopy and Quantum Chemical Calculations, *Chem. – Asian J.*, 2019, **14**(24), 4705–4711.
32 G. J. Bartlett, A. Choudhary, R. T. Raines and D. N. Woolfson, n→π* interactions in proteins, *Nat. Chem. Biol.*, 2010, **6**(8), 615–620.
33 G. Purushothaman and V. Thiruvenkatam, Analysis of intermolecular interactions in 2, 3, 5 Trisubstituted Pyrazoles derivatives: insights into crystal structures, Gaussian B3LYP/6-311G (d, p), PIXELC and Hirshfeld surface, *J. Chem. Crystallogr.*, 2016, **46**, 371–386.
34 M. Frisch, G. Trucks, H. Schlegel, G. Scuseria, M. Robb, J. Cheeseman, G. Scalmani, V. Barone, B. Mennucci and G. Petersson, *Google Scholar 2015*, Gaussian Inc, Wallingford, CT, 2009.
35 H. Burgi, J. Dunitz and E. Shefter, Geometrical reaction coordinates. II. Nucleophilic addition to a carbonyl group, *J. Am. Chem. Soc.*, 1973, **95**(15), 5065–5067.
36 A. Lari, M. B. Pitak, S. J. Coles, E. Bresco, P. Belser, A. Beyeler, M. Pilkington and J. D. Wallis, The use of the triptycene framework for observing O···C=O molecular interactions, *CrystEngComm*, 2011, **13**(23), 6978–6984.
37 S. Scheiner and T. Kar, Spectroscopic and structural signature of the CH–O hydrogen bond, *J. Phys. Chem. A*, 2008, **112**(46), 11854–11860.
38 A. v. Bondi, van der Waals Volumes and Radii, *J. Phys. Chem.*, 1964, **68**(3), 441–451.
39 V. R. Mundlapati, D. K. Sahoo, S. Bhaumik, S. Jena, A. Chandrakar and H. S. Biswal, Noncovalent Carbon–Bonding Interactions in Proteins, *Angew. Chem., Int. Ed.*, 2018, **57**(50), 16496–16500.
40 S. Saebø, F. R. Cordell and J. E. Boggs, Structures and conformations of cyclopentane, cyclopentene, and cyclopentadiene, *J. Mol. Struct.*, 1983, **104**(1–2), 221–232.
41 C. t. Altona and M. Sundaralingam, Conformational analysis of the sugar ring in nucleosides and nucleotides. New description using the concept of pseudorotation, *J. Am. Chem. Soc.*, 1972, **94**(23), 8205–8212.
42 C. A. Stortz and A. M. Sarotti, Exhaustive exploration of the conformational landscape of mono-and disubstituted five-membered rings by DFT and MP2 calculations, *RSC Adv.*, 2019, **9**(42), 24134–24145.
43 J. P. Perdew, K. Burke and M. Ernzerhof, Generalized gradient approximation made simple, *Phys. Rev. Lett.*, 1996, **77**(18), 3865.
44 S. Balasubramani, G. Chen, S. Coriani, M. Diedenhofen, M. Frank, Y. Franzke, F. Furche, R. Grotjahn, M. Harding, C. Hättig, C. vanWüllen, V. K. Voora, F. Weigend, A. Wodyński and J. M. Yu, *J. Chem. Phys.*, 2020, **152**, 184107.
45 A. Klamt, Conductor-like screening model for real solvents: a new approach to the quantitative calculation of solvation phenomena, *J. Phys. Chem.*, 1995, **99**(7), 2224–2235.
46 S. Šegan, I. Jevtić, T. Tosti, J. Penjišević, V. Šukalović, S. Kostić-Rajačić and D. Milojković-Opsenica, Determination of lipophilicity and ionization of fentanyl and its 3-substituted analogs by reversed-phase thin-layer chromatography, *J. Chromatogr. B: Anal. Technol. Biomed. Life Sci.*, 2022, **1211**, 123481.
47 G. A. Woolley, A. S. Jaikaran, Z. Zhang and S. Peng, Design of regulated ion channels using measurements of cis-trans isomerization in single molecules, *J. Am. Chem. Soc.*, 1995, **117**(16), 4448–4454.

